COMMUNICATIONS PHYSICS

ARTICLE

https://doi.org/10.1038/s42005-020-0305-7 OPEN

A novel method for stress evaluation in chemically strengthened glass based on micro-Raman spectroscopy

Nobuaki Terakado[1✉], Ryusei Sasaki[1], Yoshihiro Takahashi[1], Takumi Fujiwara[1✉], Shuji Orihara[2] & Yoshio Orihara[2]

Chemically strengthened glass is widely used for screen protection in mobile devices, and its strengthening processes and application fields have rapidly diversified. The origin of the strength is residual compressive stress induced by ion exchange, and the stress evaluation has been performed via the photoelastic effect. However, for a deep understanding of the nature of the strength and development of stronger glasses, we need a method directly connected to atomic-scale glass structures. Here, we propose a method based on the "stuffing" effect, where we can determine the residual stress non-contactively and non-destructively with a high spatial resolution using Boson, D_1, D_2, and A_1 peaks in micro-Raman spectra. Finally, we show a plausible depth dependence of the residual stress.

[1] Department of Applied Physics, Tohoku University, 6-6-05 Aoba, Aoba-ku, Sendai 980-8579, Japan. [2] Orihara Industrial, Co., Ltd., 5-47-15 Higashi-Ikebukuro, Toshima-ku, Tokyo 170-0013, Japan. ✉email: terakado@laser.apph.tohoku.ac.jp; fujiwara@laser.apph.tohoku.ac.jp

Oxide glass has become an essential industrial material owing to its advantages, such as high optical transparency, chemical durability, and formability, but at the same time, it has a critical weak point, namely, brittleness[1,2]. However, chemically strengthened glass, represented by Corning® Gorilla® Glass series, overcomes the weak point while retaining its advantages[3]. Therefore, the glass having thinness and strength becomes an indispensable material for screen protection in mobile devices such as smartphones and tablet computers, which are frequently exposed to scratches and drop impact. Also, the application of the chemically strengthened glass are now widespread, and the composition designs and strengthening processes have diversified for the development of stronger glass[4,5].

The origin of the strength of the chemically strengthened glass is residual compressive stress (CS) in the vicinity of the glass surface and the occurrence of the stress has been explained by the "stuffing" effect accompanying ion exchange[6–15]. In general, alkali-aluminosilicate glasses have been used as parent glasses, which are immersed in molten salt with alkali ions that are larger than those of the parent glasses. Then, alkali ion exchange between the parent glasses and the molten salt, e.g., Na^+ to K^+, occurs by diffusion. At this time, the immersing temperature (approximately 400 °C) is kept lower than the glass transition temperature, so that the aluminosilicate network is hardly relaxed, which leads to the compression of the glass network. This compression produces a high residual CS of up to ~1 GPa[16], resulting in high break resistance.

Two indicators, i.e., the maximal CS and the depth of layer (DOL)[3,17], are used to check the quality of the chemically strengthened glass, where the latter can be defined as the depth at which the residual stress equals zero. Conventionally, these two values are obtained from a depth profiling of stress via the photoelastic effect[18]; e.g., stress evaluation devices based on both the photoelastic effect and the waveguide effect have been commercialized and used as a standard technique. Additionally, methods using both the photoelastic effect and light scattering have been recently proposed: Using these methods, Inaba et al. succeeded in evaluating the stress in two-step ion-exchanged glass[5], and Hödemann et al. demonstrated stress detection with high spatial resolution using confocal microscopy[19].

The methods based on the photoelastic effect are suitable to conveniently determine CS and DOL, but there is also an issue, i.e., we cannot find out correlation between the CS and atomic-scale glass structures. Mostly, in the ordinary quality check of the chemically strengthened glass, it does not become problematic. However, originally, the CS should arise from the glass structures. So, it is significant that we directly evaluate the CS from the glass structures, which can lead to deep understanding of the strength by ion exchange and the development of stronger glass.

Therefore, we propose a stress evaluation method based on the "stuffing" effect. In this method, we need three structural parameters, which can be obtained from Boson, D_1, D_2, and A_1 peaks in micro-Raman spectra. In this work, we investigated a commercial chemically strengthened glass, Corning® Gorilla® Glass 3[17], which is aluminosilicate glass subjected to the ion exchange of Na^+ for K^+, and melt-quenched glasses with no residual stress whose compositions are the same as the strengthened glasses. Consequently, we show a plausible variation of the depth dependence of the residual stress. We emphasize that the present method enables the non-contact, non-destructive stress evaluation with a depth and lateral resolution on the order of microns, and moreover, there is no restriction with respect to the refractive index distribution and surface flatness, as is needed for optical waveguiding[18].

Results

Derivation of an equation for stress evaluation. The "stuffing" effect causing the CS in chemically strengthened glass has been understood by analogy with the thermal stress, i.e., the free volume expansion that is supposed to occur by ion exchange is spatially suppressed, leading to the CS[6–15]. From this viewpoint, ion exchange should correspond to the increasing temperature that creates the thermal stress. However, the free volume expansion by the ion exchange can be separated into two contributions, i.e., an intrinsic expansion by the ion exchange and an expansion by structural relaxation. It seems that the lack of this separation gives rise to a discrepancy between the theoretical and experimental values of the stress[6–15]. For an explanation of this discrepancy, a relaxation function has been adopted and anomalies with respect to the linear network dilation coefficient B and Young's modulus have been deliberated[6–15].

However, our interpretation is different from the conventional one. We consider that the structural relaxation corresponds to the increasing temperature in the process of the thermal stress, when the intrinsic expansion by ion exchange is neglected. We assume that the mean atomic volume[20] in the local strengthened area can be uniquely determined by fractional exchange s and the degree of structural relaxation r as $V(s, r)$, where $s = 0$ and 1 mean no and full exchange of alkali ions, respectively, and $r = 0$ and 1 mean no and full relaxation, respectively. Then, the residual stress σ by the "stuffing" effect is formulated as follows by analogy with the thermal stress[6–15]:

$$\sigma(s,\ r) = -\frac{E}{3(1-\nu)}\frac{V(s,\ 1) - V(s,\ r)}{V(s,\ r)} + \sigma_0. \qquad (1)$$

Here, we use V and s in the present study instead of the molar volume and the molar fraction employed in the previous studies[6–15], since V and s are appropriate for evaluations using Raman spectroscopy, as shown in the following sections. This replacement does not alter the argument of the "stuffing" effect. We use Young's modulus and Poisson's ratio of Gorilla® Glass 3 as E and ν, with ~70 GPa and ~0.2[17], respectively. Note that the equation includes just the mean atomic volume V as a variable, which determines the CS. Then, V naturally includes the structural relaxation term r and $V(s, 1)$ is the virtual value when the structure was perfectly relaxed and the stress was perfectly released. Although several origins of the structural relaxation are conceivable, it is the term r that represents the degree of structural relaxation in our approach, so that V can be uniquely determined from r and s. The parameter σ_0 is the internal tensile stress, which can be determined by the following equation of equilibrium:

$$\int_0^d \sigma(z)\mathrm{d}z = 0. \qquad (2)$$

Here, d is the sample thickness and z is the depth from the top surface of the sample. When $\sigma(z)$ is symmetric with respect to $z = d/2$, Eq. (2) becomes

$$\int_0^{d/2} \sigma(z)\mathrm{d}z = 0. \qquad (3)$$

Figure 1 shows $V(s, r)$ as a function of s and r and the schematic structures of four glasses. One glass is the parent glass α, in which we see that Na^+ ions exist in the aluminosilicate glass network. The second glass represents an "ideal" chemically strengthened state on the line segment αβ with $r = 0$, indicating that the ions are exchanged together with no structural relaxation; in other words, no changes in the topological network structures occur. The third glass is the perfectly structure relaxed glass with no "stuffing" effect, i.e., a stress of zero, on the line segment αγ with $r = 1$. The

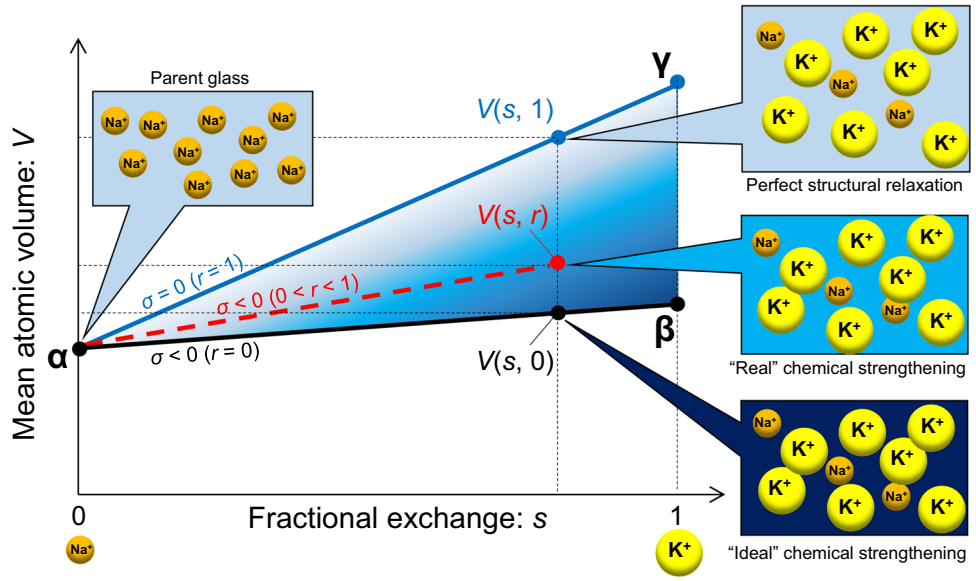

Fig. 1 Schematic illustrations of glass structures. The structures for parent glass, and "ideal" chemically strengthened, "real" chemically strengthened, and perfectly structure relaxed states, are depicted on a *V*-*s* graph.

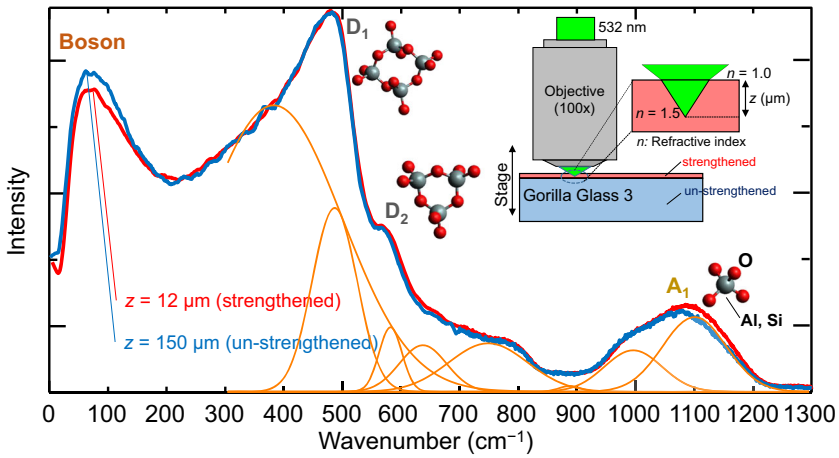

Fig. 2 Micro-Raman spectra in strengthened and un-strengthened areas of Gorilla® Glass 3. The eight Gaussian peaks that fit the spectrum (300–1300 cm^{-1}) of the un-strengthened area are also shown.

fourth glass is a local state of the "real" chemically strengthened glass, where the structure is partially relaxed. The slope of αγ is greater than that of αβ, as noted in ref. [14]. Then, assuming that an increase in r leads to a linear increase in V, $V(s, r)$ within the Δαβγ is expressed as follows:

$$V(s,r) = V_\alpha + \left[(1-r)(V_\beta - V_\alpha) + r(V_\gamma - V_\alpha)\right]s, \qquad (4)$$

where $V_\alpha = V(0, r)$, $V_\beta = (1, 0)$, and $V_\gamma = V(1, 1)$. Inserting Eq. (4) into Eq. (1), we obtain the following equation:

$$\sigma(s,r) \approx -\frac{E}{3(1-\nu)}\frac{(1-r)(V_\gamma - V_\beta)s}{V_\alpha + \left[(1-r)(V_\beta - V_\alpha) + r(V_\gamma - V_\alpha)\right]s} + \sigma_0. \qquad (5)$$

This equation suggests that the residual stress can be determined by the three parameters, V, s, and r, which are calculated from Raman spectra in this work. Calahoo et al. have already reported an evaluation of the stress in ion-exchanged lithium silicate glasses using micro-Raman spectroscopy, in which the molar volume was obtained from the bond angles and lengths in Si–O–Si[21], but it is noteworthy that we directly obtain the value of the local atomic volume from the Boson peak and we adopt the present method to the commercial chemically strengthened glass.

Raman spectra of the chemically strengthened glass. Figure 2 shows Raman spectra at $z = 12$ and 150 μm in Gorilla® Glass 3, corresponding to the chemically strengthened and un-strengthened areas, respectively (see Methods for details regarding Raman spectroscopy). The spectra show peaks that are representative of typical aluminosilicate glasses[22]. In the spectra, we focused on the four peaks, i.e., Boson (~60 cm^{-1}), D_1 (~480 cm^{-1}), D_2 (~580 cm^{-1}), and A_1 (1090–1100 cm^{-1}) peaks[22–24]. Here the Boson peak arises from acoustic modes in medium-range structure, but the origin remains controversial[25–28]. The D_1 and D_2 peaks correspond to symmetric stretching of O atoms, namely, breathing mode, in the four- and three-membered rings of TO_4 tetrahedra, respectively, where T = Al or Si[22]. The A_1 peak corresponds to an in-phase stretching of the four O atoms in TO_4 tetrahedra[22]. The reason for picking the four peaks is that we can see differences in the intensity of the D_2 peak and the peak positions of the Boson and the A_1

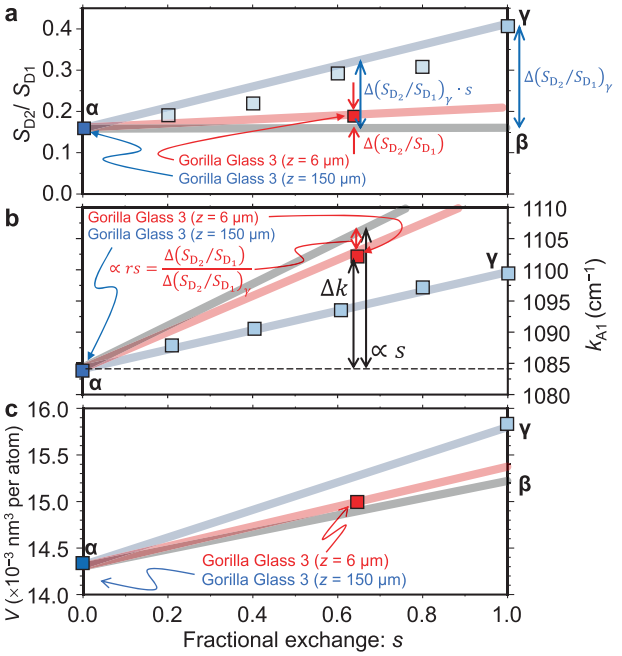

Fig. 3 Parameters derived from micro-Raman spectra as functions of the fractional exchange *s*. (**a**) Integrated area of the D_2 peak normalized by that of the D_1 peak, S_{D2}/S_{D1}, (**b**) A_1 peak positions k_{A1}, and (**c**) mean atomic volume V estimated from Eq. (9).

peaks between the spectra at $z = 12$ and 150 μm in Fig. 2 and S_{D2}/S_{D1} can be a parameter to determine the degree of structural relaxation, as explained in the next section, where S_{D2} and S_{D1} are the integrated areas of the D_2 and D_1 peaks, respectively.

Quantification of structural relaxation. First, we investigated an effect of ion exchange on the glass network in the melt-quenched glasses which are located on the line segment αγ (see Methods for details regarding the melt-quenched glasses). As a result, we found out the approximately linear relation between S_{D2}/S_{D1} and s as shown in Fig. 3a. This means that K^+ ions intrinsically prefer to coordinate to the smaller rings, comparing with Na^+ ions. Conversely, for the chemically strengthened area ($z = 6$ μm), S_{D2}/S_{D1} is as small as nearly one-fifth compared with that for the same s on the line segment αγ. This suggests that formation of the three-membered rings by exchange of Na^+ for K^+, i.e., the structural relaxation, is suppressed during the ion exchange process. Therefore, we quantify the degree of structural relaxation r as follows:

$$r = \frac{\Delta(S_{D_2}/S_{D_1})}{\Delta(S_{D_2}/S_{D_1})_\gamma \cdot s}, \tag{6}$$

where Δ denotes the difference with respect to the glass α. The subscript γ means the value is for the glass γ.

Evaluation of fractional exchange. Figure 3b shows the dependence of the A_1 peak positions k_{A1} (cm^{-1}) for the same samples as in Fig. 3a. For both types of glasses, k_{A1} increases with increasing s, in which, clearly, the value in the strengthened area is located above the line segment αγ. The reason will be discussed later; briefly, it is expected that exchange of Na^+ for the larger ions K^+ and the CS simultaneously cause an increase in k_{A1}. On the other hand, the structural relaxation causes a decrease in k_{A1}. That is, the ion exchange with no structural relaxation in the "ideal" chemically strengthened glasses shows the maximal k_{A1}, the reduction from which is attributable to the decrease by the structural relaxation. Hence, under a linear approximation, we set the following equation using two undetermined coefficients, a and b, and Eq. (6):

$$\Delta k_{A_1} = as - brs = as - b\frac{\Delta(S_{D_2}/S_{D_1})}{\Delta(S_{D_2}/S_{D_1})_\gamma}, \tag{7}$$

where a and b are determined to be 29 and 14, respectively, from the simultaneous equations for the strengthened area at $z = 6$ μm in the Gorilla® Glass 3 and the glass γ, which gives

$$s = 0.034\Delta k_{A_1} + 1.9\Delta(S_{D_2}/S_{D_1}). \tag{8}$$

Note that s can be evaluated from the A_1 and D_2 peaks in the Raman spectra using this equation.

Evaluation of mean atomic volume. The most innovative point in the present method is that we directly obtain the local mean atomic volume V in Eq. (1) using Raman spectroscopy. In the various oxide glasses, it is known that the Boson peak positions k_{BP} (cm^{-1}) are related to the mean atomic volume V (×10^{-3} nm^3/atom), although the reason has been controversial, whose relation is approximated by[25]

$$V \approx 21 - 0.11k_{BP}. \tag{9}$$

Figure 3c shows the values of V evaluated from Eq. (9), where, as anticipated in Fig. 1, the value for the γ glass is greater than that for the α glass, and the value for the strengthened area is located below the line segment αγ. The undetermined value V_β for the virtual glass β is determined to be 15.2×10^{-3} nm^3 per atom by substituting the values of V and r in the strengthened area at $z = 6$ μm in the Gorilla® Glass 3 for Eq. (4).

Evaluation of residual stress. Using Eqs. (5), (6), and (8), we obtain the equation for the residual stress in units of MPa as follows:

$$\sigma(z) \approx -30 \times 10^3 \times \frac{0.021\Delta k_{A_1} - 1.2\Delta(S_{D_2}/S_{D_1})}{14 + 0.031\Delta k_{A_1} + 4.1\Delta(S_{D_2}/S_{D_1})} + \sigma_0. \tag{10}$$

It should be emphasized that this equation does not include the term V, but the residual stress can be evaluated by only the A_1, D_1, and D_2 peaks. This is because the evaluation of V using Eq. (9) determines the undetermined parameters, V_α, V_β, and V_γ, in Eq. (5) and consequently $V(r, s)$ in Eq. (1) can be uniquely determined. In Fig. 4b–d, we show depth dependences of S_{D2}/S_{D1}, k_{A1}, and k_{BP}, respectively, in which k_{A1} and S_{D2}/S_{D1} increase and k_{BP} decreases with decreasing z when the depth is shallower than ~50 μm. Finally, we show the residual CS by comparing the estimation using Eq. (10) and the conventional surface stress meter based on the photoelastic effect and the waveguide effect, in which σ_0 was estimated to be ~40 MPa using Eq. (3). The result in the present method is in good agreement with that of the surface stress meter in terms of the magnitude of the stress, the depth dependence, and the internal tensile stress. Moreover, we observed a local stress variation at $z = 80$ and 130 μm, which may show that we succeeded in the detection of stress irregularities.

Discussion

The fact that the results from the present method are approximately equal to those from the surface stress meter is surprising, but at the same time, suggests that the present method can be valid. Here we discuss the validity of the method as below.

Regarding E and ν, we used the datasheet values[17] for Gorilla® Glass 3 in Eq. (5). These values are macroscopic values for the bulk glass, which should be used in the continuum mechanics. Therefore, the use of E and ν in Eq. (5), which is originally based

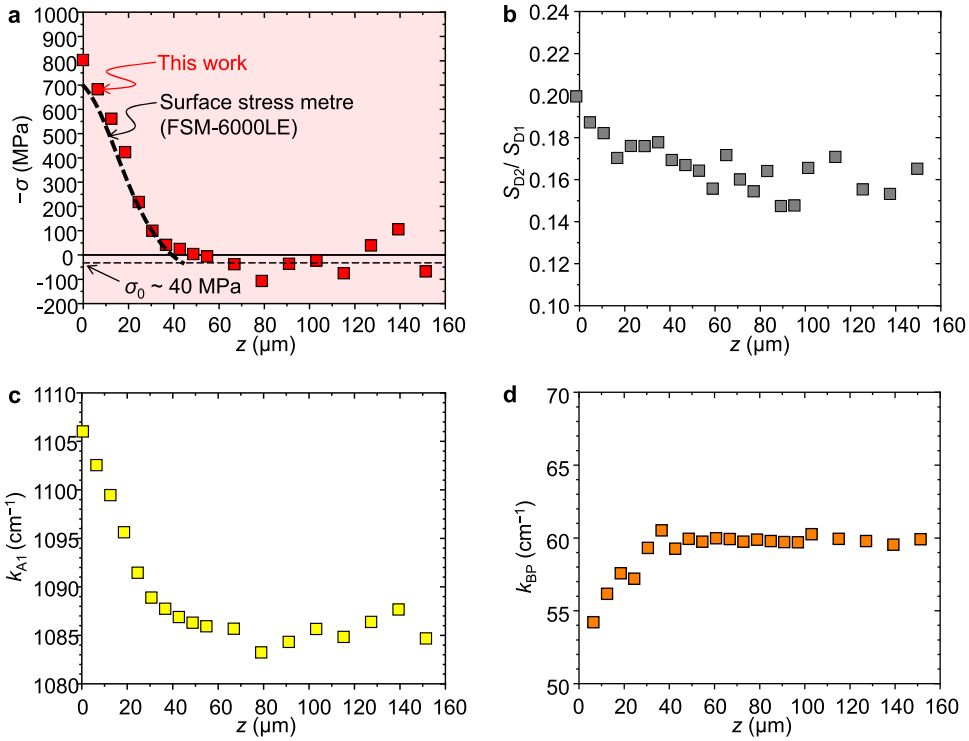

Fig. 4 Stress and parameters of Gorilla® Glass 3 drived from micro-Raman spectra as functions of the depth *z*. (**a**) Residual compressive stress obtained in this work and by using a surface stress meter, (**b**) Integrated area of the D_2 peak normalized by that of the D_1 peak, S_{D2}/S_{D1}, (**c**) A_1 peak position, k_{A1}, and (**d**) Boson peak position, k_{BP}.

on the atomic-scale structures, gives an uncertainty to Eq. (10). That is, it is unclear if E and ν in the atomic scale could be defined, and the values are expected to depend on r and s. However, attempts to evaluate E and ν from the atomic-scale structures have been performed[29,30] and the insight obtained from these researches will improve the accuracy of the stress evaluation by our method, which will enable the all-optical stress evaluation in chemically strengthened glass.

In our method, we used the melt-quenched glasses as reference state, but strictly, which also lacks accuracy. This is because the state which should be referred is "stress-free" chemically strengthened glass, which does not correspond to the melt-quenched glass, owing to different thermal or ion exchange histories. The solution may be preparation of the stress-free state by heat treatment.

For the D_1 and D_2 peak, we considered the ratio of the integrated areas as the parameter of the structural relaxation. According to Hemley et al.[31], the integrated area irreversibly increases by exposure to high pressure and subsequent releasing. This finding has been interpreted as the polymorphism of the $SiO_{4/2}$ tetrahedra network under high pressure and the subsequent formation of the three-membered rings, being the origin of the D_2 peak. On the basis of this picture, coincidentally recalling that K^+ ions prefer to coordinate to the small rings, we can naturally understand the increase in the intensity in the strengthened area in Fig. 3a, i.e., the ion exchange induces a high stress in the local area of the glass, but coincidently, the high immersing temperature under ion exchange promotes the stabilization of the $TO_{4/2}$ network in conjunction with the high stress, when it is expected that network polymorphism and the subsequent formation of the three-membered rings partially occur.

We used the linearity assumption in Eq. (4). The validation of the assumption is an important and controversial problem. Although it is not sufficient to explain the linearity, we have an atomic-scale picture: we obtain the following equation from Eqs. (4) and (6):

$$V\left(s,\Delta(S_{D_2}/S_{D_1})\right)=V_\alpha+\left[s(V_\beta-V_\alpha)+\frac{\Delta(S_{D_2}/S_{D_1})}{\Delta(S_{D_2}/S_{D_1})_\gamma}(V_\gamma-V_\beta)\right]. \tag{11}$$

This equation means that an increase in the smaller rings together with the structural relaxation causes a linear increase in the mean atomic volume. This picture and the linearity assumption in Eq. (4) is correct, assuming that S_{D2}/S_{D1} is linearly proportional to volume fraction of the structural relaxed area. The validity of this assumption remains unclear, which also reduces the accuracy of the stress evaluation.

The linear approximation for the A_1 peak position, Eq. (7), originally comes from the following relation:

$$\Delta k_{A_1}(s,r)\approx r\Delta k_{A_1}(s,1)+(1-r)\Delta k_{A_1}(s,0)\,. \tag{12}$$

In this equation, $\Delta k_{A1}(s, 0)$ and $\Delta k_{A1}(s, 1)$ are changes with respect to the glass α in the "ideal" chemically strengthened and the perfectly structure relaxed glasses, respectively. Considering that $\Delta k_{A1}(s, 1)$ comprises two contributions of the Na^+ ion exchange for K^+ and the formation of the small rings, defined as $\Delta k_{A1}(s, 1)_{Na^+\to K^+}$ and $\Delta k_{A1}(s, 1)_{SR}$, respectively, Eq. (12) is rewritten as follows in terms of *s*:

$$\begin{aligned}\Delta k_{A_1}(s,r)&\approx\Delta k_{A_1}(s,0)-\left(\Delta k_{A_1}(s,0)-\Delta k_{A_1}(s,1)_{Na^+\to K^+}-\Delta k_{A_1}(s,1)_{SR}\right)r\\&\approx\frac{\partial k_{A_1}(s,0)}{\partial s}s-\left(\frac{\partial k_{A_1}(s,0)}{\partial s}-\frac{\partial k_{A_1}(s,1)_{Na^+\to K^+}}{\partial s}-\frac{\partial k_{A_1}(s,1)_{SR}}{\partial s}\right)rs.\end{aligned} \tag{13}$$

The second line in Eq. (13) is qualitatively consistent with Eq. (7). Quantitatively, we may be able to explain the behaviors on the basis of the central-force model[31–33]. This model approximately

gives the following relation to the A_1 peak position:

$$\omega_{A_1}^2 \approx \frac{\alpha}{m}(1-\cos\theta), \quad (14)$$

where $\omega_{A1} = ck_{A1}$, c is the light speed, α is the restoring force constant of the T–O bond, m is the mass of oxygen, and θ is the bond angle of T–O–T. Considering a small change with respect to the glass α, Eq. (14) becomes

$$\frac{1}{k_{A_1,\alpha}}\frac{\partial k_{A_1}}{\partial s} \approx \frac{1}{2\alpha_\alpha}\frac{\partial \alpha}{\partial s} + \frac{\sin\theta_\alpha}{1-\cos\theta_\alpha}\frac{\partial \theta}{\partial s}. \quad (15)$$

In Fig. 3b, we see that the chemically strengthened glass shows a notable shift to a higher wavenumber compared with the melt-quenched glass. This shift is because $\partial k_{A1}(s, 0)/\partial s$ in Eq. (13), i.e., a in Eq. (7), is dominantly positive. In the case of SiO_2 glass, according to Weigel et al.[33], when the glass is pressurized using a penetrating medium, He, α increases and a decrease in θ is suppressed. Then, the term of $\partial\alpha/\partial p$ (p: pressure), which corresponds to $\partial\alpha/\partial s$ in Eq. (15), becomes dominant, leading to a shift in k_{A1} to a higher wavenumber. The same scenario can be established in the ion exchange process. On the other hand, the quantitative interpretation of the coefficient of rs in Eq. (13), i.e., b in Eq. (7), seems to be puzzling at present. For a further understanding of the structural relaxation, determination of α and θ by adopting the central-force model and the modified one to the peaks, including R band (~380 cm^{-1}) etc. is helpful[33,34].

Let us consider whether this approach is applicable to other chemically strengthened glasses having different compositions from Gorilla® Glass 3. To get to the point, we think the answer is yes if Eq. (1) is satisfied and the three parameters can be obtained from Raman spectra, when the empirical coefficients in Eq. (10) should depend on the glass composition because r and s dependences of V should be affected by the composition. In the case of the two-step ion exchange process, which is the standard one in the present day for giving deeper DOL, one solution is replacement of $V(r, s)$ with $V(r, s_1, s_2)$, where, for example, s_1 and s_2 are fractional exchange for Na^+ and K^+, respectively, for Li^+-based pristine glass. Then, the V-s plane in Fig. 1 is extended to a V-s_1-s_2 space, and the observation point by the Raman spectroscopy corresponds to a point in the space.

In summary, we proposed a method to evaluate the CS of the chemically strengthened glass, which is directly connected to the atomic-scale structures. The method is based on the "stuffing" effect and the micro-Raman spectroscopy and enables the non-contact, non-destructive stress evaluation with a depth and lateral resolution on the order of microns, without restriction with respect to the refractive index distribution and surface flatness. Although the method needs several linear assumptions for the structural change by ion exchange and relaxation and the macroscopic values, E and ν, which reduces the accuracy of the stress evaluation, we obtained the plausible result in good agreement with that of the surface stress meter in terms of the magnitude of the stress, the depth dependence, and the internal tensile stress.

Methods

Sample preparation and characterization. The samples used were two types of oxide glasses. One sample was the commercial chemically strengthened glass, Corning® Gorilla® Glass 3. The glasses before and after ion exchange were purchased. The version of the glasses was not the latest but were suitable for the present study because they were expected to possess the conventional aluminosilicate network. Using a wavelength dispersive X-ray fluorescence spectrometer (XRF; S8 Tiger, Bruker, USA), the composition of the Gorilla® Glass before the ion exchange was determined approximately to be $16Na_2O$–$13Al_2O_3$–$69SiO_2$–$0.3MgO$–$0.01SnO_2$ in mol%. On the basis of this composition, the glasses which have compositions of $16(1-s)Na_2O$–sK_2O–$13Al_2O_3$–$69SiO_2$–$0.3MgO$–$0.01SnO_2$ ($s = 0.2$, 0.4, 0.6, 0.8, and 1.0) were prepared by a melt-quenching method: NaOH, KOH, Al_2O_3, SiO_2, MgO, and SnO_2 reagents with purities over 99.9% were used. Their powders were weighed and mixed to obtain the above compositions. The batches were placed in a platinum crucible and melted at 1650 °C for 1 h in air using an electric furnace at a heating rate of 10 °C/min. The melts were quenched in a furnace maintained at 500 °C and were subsequently removed from the furnace.

The fractional exchange s in the ion-exchanged area of Gorilla® Glass 3 was obtained by a scanning electron microscope equipped with energy dispersive X-ray spectroscopy (EDX; JSM-6500F, JEOL, Japan). Note that we did not add Li_2O and B_2O_3 to the compositions based on XRF so that these compositions were compared with those of EDX, in which Li and B, being light elements, could not be detected, although there is a possibility that the chemically strengthened glass contains a few mol% of these contents.

A depth profile of CS in Gorilla® Glass 3 was obtained by using a surface stress meter (FSM-6000LE, Orihara Industrial, Japan) for comparison with the result in this work.

Raman spectroscopy. Raman spectra of the samples were obtained using a conventional system (NRS-5500, JASCO, Japan). The system included confocal microscopy with a 100× objective lens with a numerical aperture (NA) of 0.9 and an excitation source of 532-nm laser light. The scattered light was detected with a backscattering configuration when the light incident to the samples was linearly polarized, while the scattered light was detected with no polarizer. The depth and lateral resolutions were approximately 2 and 1 μm, respectively. We obtained a depth (z) dependence of the Raman spectra, where z is a depth from the top surface of the glass plate, namely, an actual focus position, and has been compensated by refractive index of the sample. Here the index is assumed to be 1.5, being independent of z, and this assumption is reasonable because the values of the index are reported to be 1.50 and 1.51 (for 590-nm light) for the un-strengthened and the chemically strengthened areas of Gorilla® Glass 3, respectively[17]. The spectra in a range of 300–1300 cm^{-1} were deconvoluted by eight Gaussian peaks, which are located at ~380, ~480, ~580, ~640, ~750, ~890, 980–1000, and 1090–1100 cm^{-1}, as shown in Fig. 2. The assignment of each peak is described in refs. [22,24]. For the Boson peak at ~60 cm^{-1}, following the conventional analysis method[25,35–38], the peak position was determined by fitting with the log-normal distribution function for the Raman intensity at 30–120 cm^{-1} reduced by the Bose factor.

Data availability

The authors declare that the data supporting the findings of this study are available within the article.

Received: 13 June 2019; Accepted: 4 February 2020;
Published online: 21 February 2020

References

1. Taylor, N. W. Mechanism of fracture of glass and similar brittle solids. *J. Appl. Phys.* **18**, 943–955 (1947).
2. Adams, R. & McMillan, P. W. Static fatigue in glass. *J. Mater. Sci.* **12**, 643–657 (1977).
3. Corning Gorilla Glass 6 Product information sheet. Available at https://www.corning.com/microsites/csm/gorillaglass/PI_Sheets/Corning_Gorilla_Glass_6_PI_Sheet.pdf
4. Green, D. J., Tandon, R. & Sglavo, V. M. Crack arrest and multiple cracking in glass through the use of designed residual stress profiles. *Science* **283**, 1295–1297 (1999).
5. Inaba, S., Ogami, S., Orihara, S. & Orihara, Y. Non-destructive stress measurement in double ion-exchanged glass using optical guided-waves and scattered light. *J. Ceram. Soc. Jpn.* **125**, 814–820 (2017).
6. Gy, R. Ion exchange for glass strengthening. *Mater. Sci. Eng. B* **149**, 159–165 (2008).
7. Macrelli, G. Chemically strengthened glass by ion exchange: strength evaluation. *Int. J. Appl. Glass Sci.* **9**, 156–156 (2017).
8. Cooper, A. R. & Krohn, D. A. Strengthening of glass fibers: II, Ion exchange. *J. Am. Ceram. Soc.* **52**, 665–669 (1969).
9. Bartholomew, R. F. & Garfinkel, H. M. in *Glass: Science and Technology* (eds Uhlmann, D. R. & Kreidl, N. J.) Vol. 5, 217–270 (Academic Press, New York, 1980).
10. Sane, A. Y. & Cooper, A. R. Stress buildup and relaxation during ion exchange strengthening of glass. *J. Am. Ceram. Soc.* **70**, 86–89 (1987).
11. Shen, J. & Green, D. J. Prediction of stress profiles in ion exchanged glasses. *J. Non-Cryst. Solids* **344**, 79–87 (2004).
12. Varshneya, A. K. Chemical strengthening of glass: lessons learned and yet to be learned. *Int. J. Appl. Glass Sci.* **1**, 131–142 (2010).
13. Varshneya, A. K. The physics of chemical strengthening of glass: room for a new view. *J. Non-Cryst. Solids* **356**, 2289–2294 (2010).
14. Vargheese, K. D., Tandia, A. & Mauro, J. C. Molecular dynamics simulations of ion-exchanged glass. *J. Non-Cryst. Solids* **403**, 107–112 (2014).

15. Varshneya, A. K., Olson, G. A., Kreski, P. K. & Gupta, P. K. Buildup and relaxation of stress in chemically strengthened glass. *J. Non-Cryst. Solids* **427**, 91–97 (2015).
16. See, for example, Murayama, S., Ohara, S., Li, Q. & Akiba, S., WO 2017/126607 A1 (2017).
17. Corning Gorilla Glass 3 Product information sheet. Available at https://www.corning.com/microsites/csm/gorillaglass/PI_Sheets/CGG_PI_Sheet_Gorilla%20Glass%203.pdf.
18. Kishii, T. Surface stress meters utilizing the optical waveguide effect of chemically tempered glasses. *Opt. Laser Eng.* **4**, 25–38 (1983).
19. Hödemann, S. et al. Confocal detection of Rayleigh scattering for residual stress measurement in chemically tempered glass. *J. Appl. Phys.* **118**, 243103 (2015).
20. Soga, N., Yamanaka, H., Hisamoto, C. & Kunugi, M. Elastic properties and structure of alkaline-earth silicate glasses. *J. Non-Cryst. Solids* **22**, 67–76 (1976).
21. Calahoo, C., Zwanziger, J. W. & Butler, S. Mechanical-structural investigation of ion-exchanged lithium silicate glass using micro-Raman spectroscopy. *J. Phys. Chem. C* **120**, 7213–7232 (2016).
22. Losq, L., Neuville, D. R., Florian, P., Henderson, G. S. & Massiot, D. The role of Al^{3+} on rheology and structural changes in sodium silicate and aluminosilicate glasses and melts. *Geochim. Cosmochim. Acta* **126**, 495–517 (2014).
23. Terakado, N., Uchida., S., Takahashi, Y., Fujiwara, T. & Arakawa, M. Depth analysis of a compression layer in chemically strengthened glass using depth-resolved micro-Raman spectroscopy. *J. Ceram. Soc. Jpn.* **124**, 1164–1166 (2016).
24. Terakado, N., Uchida, S., Sasaki, R., Takahashi, Y. & Fujiwara, T. CO2 laser-induced weakening in chemically strengthened glass: Improvement in processability and its visualization by Raman mapping. *Ceram. Int.* **44**, 2843–2846 (2018).
25. Nakamura, K., Takahashi, Y., Osada, M. & Fujiwara, T. Low-frequency Raman scattering in binary silicate glass: boson peak frequency and its general expression. *J. Ceram. Soc. Jpn.* **121**, 1012–1014 (2013).
26. Shintani, H. & Tanaka, H. Universal link between the boson peak and transverse phonons in glass. *Nat. Mater.* **7**, 870 (2008).
27. Kojima, S. et al. Boson peaks of lithium borate glasses studies by inelastic neutron and light scattering. *J. Non-Cryst. Solids* **356**, 2524 (2010).
28. Marruzzo, A., Schirmacher, W., Fratalocchi, A. & Ruocco, G. Heterogeneous shear elasticity of glasses: the origin of the Boson peak. *Sci. Rep.* **3**, 1407 (2013).
29. Makishima, A. & Mackenzie, J. D. Direct calculation of Young's modulus of glass. *J. Non-Cryst. Solids* **12**, 35–45 (1973).
30. Rouxel, T., Ji, H., Keryvin, V., Hammouda, T. & Yoshida, S. Poisson's ration and the glass network topology – Relevance to high pressure densification and indentation behaviour. *Adv. Mater. Res.* **39–40**, 137–146 (2008).
31. Hemley, R. J., Mao, H. K., Bell, P. M. & Mysen, B. O. Raman spectroscopy of SiO2 glass at high pressure. *Phys. Rev. Lett.* **57**, 747–750 (1986).
32. Sen, P. N. & Thorpe, M. F. Phonons in AX2 glasses: from molecular to band-like modes. *Phys. Rev. B* **15**, 4030–4038 (1977).
33. Weigel, C. et al. Polarized Raman spectroscopy of v-SiO_2 under rare-gas compression. *Phys. Rev. B* **93**, 224303 (2016).
34. Li, Y. et al. Surface molecular structure defects and laser-induced damage threshold of fused silica during a manufacturing process. *Sci. Rep.* **7**, 17870 (2017).
35. Shunker, R. & Gammon, R. W. Raman-scattering selection-rule breaking and the density of states in amorphous materials. *Phys. Rev. Lett.* **25**, 222 (1970).
36. Shimodaira, N., Saito, K., Hiramitsu, N., Matsushita, S. & Ikushima, J. Effects of fictive temperature and halogen doping on the boson peak in silica glass. *Phys. Rev. B* **71**, 024209 (2005).
37. Takahashi, Y., Osada, M., Masai, H. & Fujiwara, T. Anomalous Boson behavior and nanometric heterogeneity in glass fresnoite. *Appl. Phys. Express* **1**, 121902 (2008).
38. Takahashi, Y., Osada, M., Masai, H. & Fujiwara, T. Crystallization and nanometric heterogeneity in glass: In situ observation of the boson peak during crystallization. *Phys. Rev. B* **79**, 214204 (2009).

Acknowledgements

This work was partially supported by JSPS KAKENHI Grant Number 16K14087. We thank JASCO Corporation for supporting the Raman spectroscopy work. We thank Dr. Kensaku Nakamura and Mr. Shohei Uchida for sample preparation and characterization.

Author contributions

R.S. and N.T. fabricated and characterized the materials. S.O. and Y.O. performed the stress evaluation by the surface stress meter. N.T., T.F., R.S., and Y.T. designed the work. N.T. wrote the manuscript.

Competing interests

The authors declare no competing non-financial interests but the following competing financial interests: N.T., T.F., Y.T., and R.S. are co-inventors of a pending patent relating to the method described in the manuscript. S.O. and Y.O. belong to Orihara Industrial, Co., Ltd., which develops and markets stress evaluation equipment including the surface stress meter referred to in the manuscript.

Additional information

Supplementary information is available for this paper at https://doi.org/10.1038/s42005-020-0305-7.

Correspondence and requests for materials should be addressed to N.T. or T.F.

Reprints and permission information is available at http://www.nature.com/reprints

Publisher's note Springer Nature remains neutral with regard to jurisdictional claims in published maps and institutional affiliations.